Proceedings of the 20th International Conference on Soil Mechanics and Geotechnical Engineering– Rahman and Jaksa (Eds)
© 2022 Australian Geomechanics Society, Sydney, Australia, ISBN 978-0-9946261-4-1

Numerical analysis of a segmented tunnel lining subjected to regional consolidation

Analyse numérique d'un revêtement de tunnel segmenté soumis à une consolidation régionale

Sergio A. Martínez-Galván, Juan M. Villagrán-Alegría
SEPI, ESIA Zacatenco, IPN, Mexico City, Mexico, samartinezg@ipn.mx

Moisés Juárez-Camarena
Geotechnics, Instituto de Ingeniería, UNAM, Mexico

ABSTRACT: Paper deals with the assessment of changes of stresses and deformations of a segmented tunnel lining (primary) induced by differential settlement along tunnel that in turn is generated by regional consolidation process (subsidence) and by distance between tunnel base and the underlying hard layer. Segmented tunnel lining and subsoil are modeled using finite differences method, simulating the regional consolidation process due to drawdown of pore pressure profile. Furthermore, translations and rotations between segments and between rings are calculated by the model, when considering longitudinal and transversal joints and transition joints of the lining-soil contact. The joints are modeled by normal stiffness and shear stiffness. The regional consolidation periods considered are 2, 5 and 15 years of tunnel service. The site stratigraphy is constituted by soft clay formation with high compressibility and low shear strength and underlying hard layer close to the tunnel base composed by very compact silty sand. Results show that, to short periods, in this study, up to 5 years of regional consolidation there are no significant increases in stress and deformations in the segmented tunnel lining, and that the translations and rotations between segments and between rings are not important either.

RÉSUMÉ : L'article traite de l'évaluation des changements de contraintes et de déformations d'un revêtement (primaire) de tunnel segmenté induit par le tassement différentiel le long du tunnel qui à son tour est généré par le processus de consolidation régionale (affaissement) et par la distance entre la base de tunnel et la couche duré sous-jacente. Le revêtement et le sous-sol du tunnel segmenté sont modélisés à l'aide de la méthode des différences finies, simulant le processus de consolidation régionale dû au rabattement du profil de pression interstitielle. De plus, les translations et rotations entre segments et entre anneaux sont calculées par le modèle, en considérant les joints longitudinaux et transversaux et les joints de transition du contact revêtement-sol. Les articulations sont modélisées par la rigidité normale et la rigidité au cisaillement. Les périodes de consolidation régionales considérées sont de 2, 5 et 15 ans de service du tunnel. La stratigraphie du site est constituée d'une formation d'argile molle avec une compressibilité élevée et une faible résistance au cisaillement et une couche dure sous-jacente proche de la base du tunnel composée de sable limoneux très compact. Dans cette étude, les résultats montrent que, sur de courtes périodes, jusqu'à 5 ans de consolidation régionale, il n'y a pas d'augmentation significative des contraintes et des déformations dans le revêtement du tunnel segmenté, et que les translations et rotations entre les segments et entre les anneaux ne sont pas non plus importantes.

KEYWORDS: joints, stiffness, regional consolidation, uniform ring, segmented lining.

1 INTRODUCTION

Tunnels commonly present one or two lining, primary and secondary. The first one based on precast segments and the second one based on cast-in-place concrete. The secondary lining is generally constructed to ensure the long-term performance of tunnel. This paper considers to the tunnel with only the primary lining, this is the most critical consideration due to is not a uniform ring. Figure 1 shows the longitudinal joints, JL, (segment-segment contact) and transverse joints, JT, (ring-ring contact). Aim of this paper is to assessment the stability by deformation generated in the primary lining of a tunnel subjected to regional consolidation, where several periods of regional consolidation are considered, from 2 years to 15 years.

In several investigations on the stability of segmented tunnels lining, the geotechnical analysis of the tunnel is modeled as a uniform ring, without longitudinal joints and without transverse joints, however, the stiffness of the uniform ring is higher than the stiffness of the segmented tunnel, so normally this procedure involves using a stiffness reduction factor, to equalize the behavior of the continuous ring with that of a segmented ring. This is achieved by reducing the stiffness of the uniform ring in the geotechnical analysis, until reaching a stiffness equivalent to that of the structural analysis (Comulada-Simpson M. & Maidl, 2010). The process consists of calibrating the geotechnical analysis with the structural analysis, in terms of ring deformation, by interactively varying in the geotechnical analysis, the stiffness of the uniform ring, each interaction providing a new state of stresses acting on the ring, which is applied in the structural analysis until a similar convergence between geotechnical and structural analysis is reached, thus, the corresponding stress and deformation states are calibrated between the two models.

Segmented tunnel lining and subsoil are modeled using finite differences method, Flac^{3D} software (Itasca, 2011), simulating the regional consolidation process due to drawdown of pore pressure profile. Furthermore, translations and rotations between segments and between rings are calculated by the model, when considering longitudinal joints (segment-to-segment contact), transversal joints (ring-to-ring contact) and transition joints of the lining-soil contact. The joints are modeled by normal stiffness and shear stiffness. The regional consolidation periods considered are 2, 5 and 15 years of tunnel service. Three consecutive rings are analyzed.

1.1 *Tunnel geometry*

The tunnel under study has a circular section with an outer diameter of 10 m, it is formed by a single lining consisting of 6+1 precast concrete segments, the thickness of the segments is 0.40 m and a width of 1.50 m. The geometric center of the tunnel is at depths of 20, 25 and 27.5 m (Figure 2), so it has a cover of 15, 20 and 22.5 m thick, respectively. The primary lining is composed of a total of 7 segments, six of equal length and a closing or cutting segment (segment k), six segments have an arc length comprised in an angle θ of 55° and segment k has an arc length comprised in an angle α of 30°. Figure 1 shows the orientation of the longitudinal joints and location of segment k in the geometric model. Parameters and dimensions of the concrete segments used in the numerical analyses are listed in Table 1.

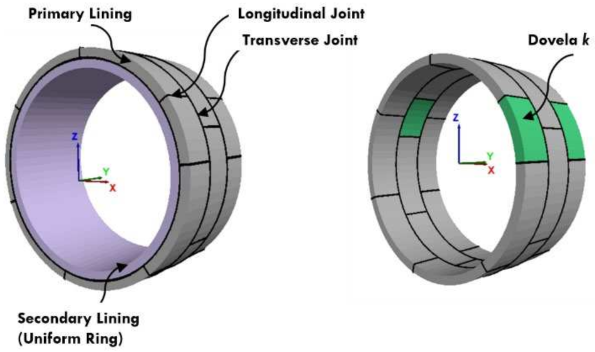

Figure 1. a) Primary and secondary lining b) keystone orientation k.

Table 1. Parameters of the concrete liner segments.

Parameter	Segment
Volumetric weight, γ (kN/m^3)	24.0
Deformation modulus, E (GPa)	21.70
Poisson's ratio, υ (---)	0.20
Compressive strength, f´c (MPa)	35

2 CASES TO ANALYZE

Three cases of analysis are established, in order to assess the critical distance between the base of the tunnel and the underlying hard layer, since the most critical condition of analysis is when the tunnel base makes contact with the hard layer (Rodríguez, 1983), this distance is evaluated so that the deformation approaches the deformation limit of the segmented lining, three distances from the level of the underlying hard layer to the base of the tunnel are proposed: 2.50 m case I, 5.0 m case II, and 10.0 m case III. Figure 2 illustrates the three cases mentioned.

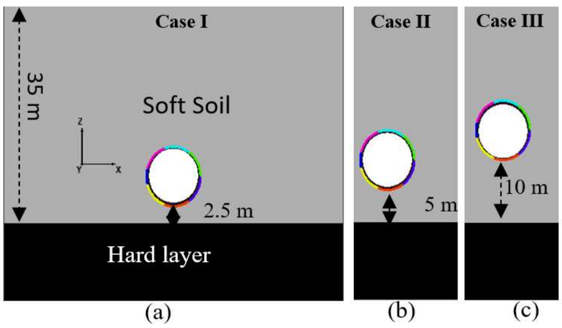

Figure 2. Distance from the hard layer to the bottom of the tunnel. a) Case I. b) Case II. c) Case III.

Only the distances from the hard layer to the tunnel base are varied, the properties of the soil and the hard layer are similar in the three cases. Likewise, the same distribution of elements is used in the numerical model in all three cases to avoid reducing the meshing effect.

2.1 *Stratigraphic characteristics and design parameters*

The stratigraphy is formed by high plasticity clays (unit A, CH) of soft consistency and low shear strength, below this soft soil underlies a hard layer formed by very compact silty sand (unit B, SM). Tables 2 and 3 show the thicknesses of layers and the strength, deformation and compressibility parameters considered to soil substrata, for short and long term in the analysis of interaction soil-lining.

Table 2. Strength, deformation, and compressibility parameters used in the short-term analysis.

Material	Clay formation					Hard layer
Parameter	A1	A2	A3	A4	A5	B
Depth (m)	0-3	3-9	9-18	18-30	30-35	35-47.5
Volumetric weight, γ (kN/m^3)	12.0	12.0	12.0	12.0	12.0	18.0
Undrained cohesion, c (kPa)	11.5	13.0	15.4	26.9	50.0	200.0
Undrained angle of internal friction, ϕ (degrees)	0.0	0.0	0.0	0.0	0.0	35.0
Undrained deformation modulus, E (kPa)	800	1,000	1,400	1,800	3,500	15,000
Undrained Poisson's ratio, υ (---)	0.49	0.49	0.49	0.49	0.49	0.30
Coefficient of earth pressure at rest, K_0 (---)	0.54	0.54	0.54	0.54	0.54	0.43

Table 3. Compressibility parameters used in the long-term analysis.

Material	Clay formation				
Parameter	A1	A2	A3	A4	A5
Initial void ratio, e_0 (---)	5.0	4.7	4.5	4.3	3.9
Lambda, λ (---)	1.89	2.03	2.21	2.19	1.42
Kappa, κ (---)	0.41	0.23	0.17	0.18	0.07
Compression coefficient, C_C (---)	4.36	4.68	5.09	5.04	3.28
Recompression coefficient, C_s (---)	0.95	0.54	0.40	0.41	0.15
Over-consolidation ratio, OCR (---)	1.11	1.14	1.18	1.25	1.31
Effective angle of internal friction, ϕ' (degrees)	35.0	35.0	35.0	35.0	35.0
Effective Poisson's ratio, υ' (---)	0.30	0.30	0.30	0.30	0.30

2.2 *Piezometric conditions and initial stress state*

The initial subsoil pore pressures considered are hypothetical, but representative of sites in the lake zone of Mexico City. The piezometric profile considers that the NAF (groundwater level) is located on the land surface, Figure 3. The same figure shows respectively the projection of the piezometric abatement for 2, 5 and 15 years of deep pumping, estimated projections from the water flow calculation for the considered stratigraphy and the piezometric initial conditions, also considered.

3 INTERACTION SOIL-TUNNEL LINING

3.1 *Three-dimensional finite-difference model*

To simulate the excavation and regional consolidation process, a three-dimensional finite difference model is developed, Figure 4. The mesh is 47.50 meters high, 60 meters wide and 4.50 meters long, it is made up of 60,048 three-dimensional zones, which in turn form tetrahedral elements. The elements of the segments in the xz-axis are distributed every 5 degrees and longitudinally (y-axis) the segments are distributed in 4 elements of 0.375 meters. The meshing and tetrahedral elements characteristics are similar for the three cases where the segmental tunnel presents a free condition at its ends.

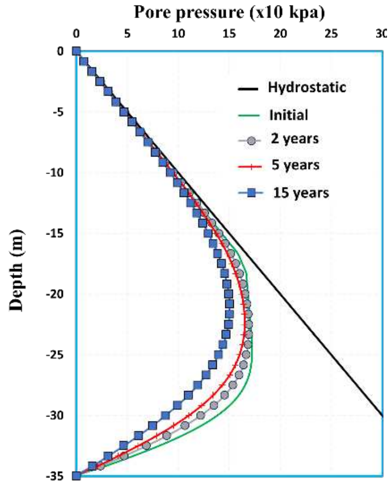

Figure 3. Initial pore pressure profile and 2, 5 and 15 years of piezometric abatement, approx.

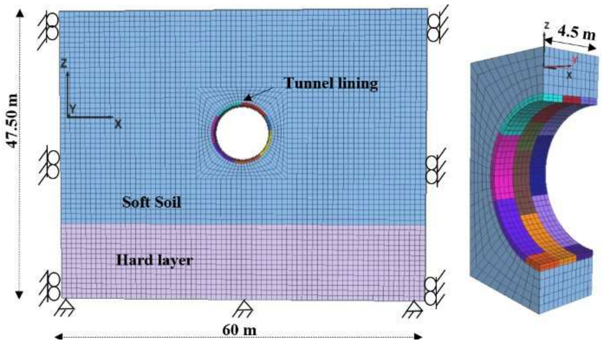

Figure 4. Three-dimensional model for the three cases (I, II, III).

3.2 *Stiffness definition of the interface set*

A parametric analysis is carried out to determine the normal stiffness kn and shear stiffness ks of the transverse (ring-ring contact), longitudinal (segment-segment contact) and transition (soil-lining contact) joints, Figure 5. To justify the parameters used in the excavation and consolidation analyses.

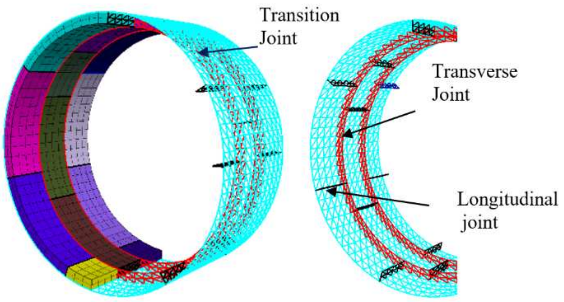

Figure 5. Longitudinal, transverse and transition joints.

Also, to calibrate the displacements between segments after excavation, the present work considers the following criteria for a tunnel lining with an inner diameter of 9.20 m (DAUB, 2013):

a) Relative displacement between segments after excavation should not exceed 0.38 mm.

b) The angular deviation (separation) between segments after excavation should be less than 0.58 mm.

c) Results: Figures 6 and 7 show respectively, the variation of the normal and shear displacements, as a function of the stiffness of the interface set. Table 4 summarizes the values of the stiffness of the interface set considered in the analysis of the soil-tunnel lining interaction. The same table includes the transition joint (JS) that considers the cohesion and friction characteristics of the soil, soil-lining contact.

3.3 *Additional considerations*

In addition to the geometry and stiffness of the interfaces, the analysis procedure considers:

a) The excavation analysis is realized with soil parameters in the short term (undrained conditions, Table 2). The excavation and placement of the lining are carried out in the same stage.

b) To piezometric abatements greater than two years, the analysis is realized to volume changes (drained conditions). The pore pressure dissipation generated by the excavation is achieved shortly after the laying of the liner (Gutiérrez and Schmitter, 2010).

c) Mortar injected in the clearance between the liner and the cutterhead skirt is not considered.

d) The axial force on the rings generated during excavation by the equipment, jacks, is not considered, which makes an unfavorable condition, since the axial force provides a better load resisting capacity to the lining (Galván, 2013), which translates into a higher longitudinal stiffness of the tunnel.

e) Tangential forces generated by the installation of the closing segment or segment k, which results in a higher tangential stiffness of the rings, are not considered.

f) Decrease in the modulus of elasticity of concrete due to plastic flow is not considered.

g) The calculated deformations in the interface elements linking ring to ring decrease the longitudinal forces applied by the jacks during tunnel construction, so the stiffness adopted in this work is not far from that occurring during the consolidation stage of the soil confining to the tunnel.

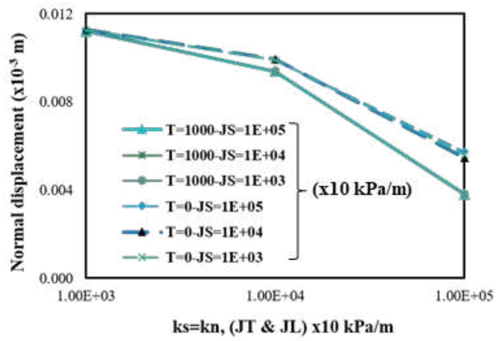

Figure 6. Normal displacements (openings) between segments.

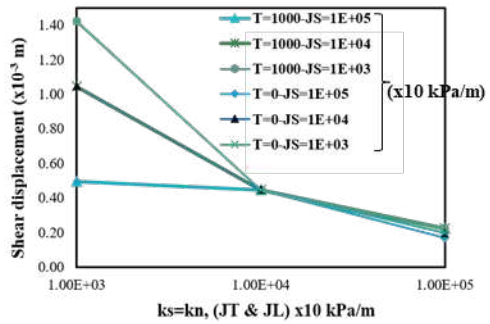

Figure 7. Tangential displacements between segments.

Table 4. Stiffness of the interface set considered in the analysis of the soil-tunnel lining interaction.

Transversa joint, JT (kPa/m)	Longitudinal joint, JL (kPa/m)	Transition joint, JS (kPa/m)	Tension strength, T (kPa/m)
$k_n = k_s$	$k_n = k_s$	$k_n = k_s$	----
1.00E+06	1.00E+06	1.00E+05	0

$k_s =$ shear stiffness, $k_n =$ normal stiffness

3.4 *Deformations for each analysis stage*

For the cases analyzed, respectivaly, the Figures 8, 9 and 10 show the vectorial norm of displacement calculated in the tunnel lining, only the second ring, caused by excavation and for the periods of piezometric abatement considered (2, 5 y 15 years). The cited figures show:

a) As reference to the deformed lining calculated in each case, the dotted line circle indicated as lining is arbitrarily located at 0.10 m on the x-y axes, from that position, the calculated displacements are added or subtracted.

b) All the cases analyzed show oval, convergence of top-heading and bottom and divergence of the sides.

c) By modeling the excavation, a lift of the liner is observed.

d) The consolidation process causes the tunnel to descend, and the sides tend to open.

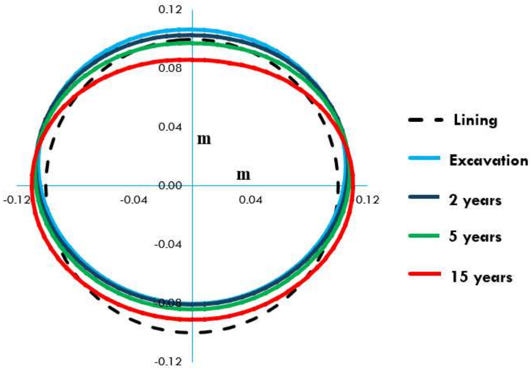

Figure 8. Comparison of lining deformated (m) for case I.

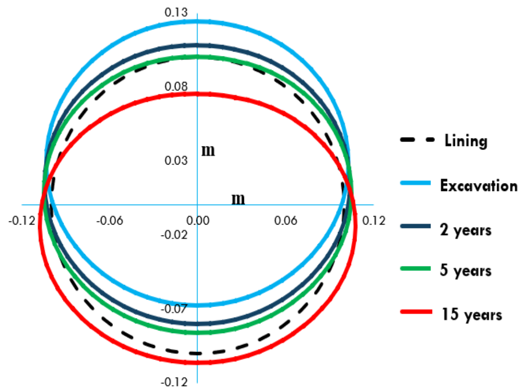

Figure 9. Comparison of lining deformated (m) for case II (m).

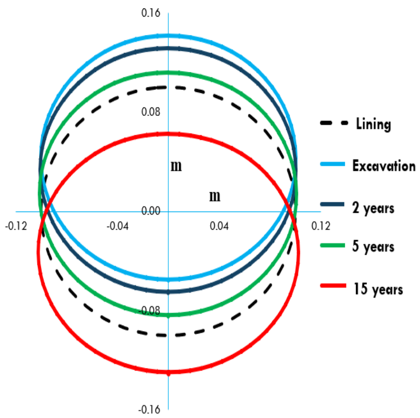

Figure 10. Comparison of lining deformated (m) for case III.

3.5 *Mechanical elements in the tunnel lining*

The bending moment calculated are compared with the results published by Zhenchang *et al*. (2015), when he considers a ring with outer diameter of 6.2 m, composed of 1 key segment (segment k), 2 adjacent segments and 3 standard segments. Figure 11 shows the bending moment along the lining perimeter of that investigation and results of the present study, but for a segmented ring with high stiffness at the interfaces, to assessment the analysis procedure used. Where η it the effective ratio of bending rigidity, ξ it the transfer ratio of bending moment, k_r^+/k_r^- it the stiffness of rotation spring, k_s it the stiffness of shear spring. Figure includes a diagram illustrating the reference angle variation θ. Graphs in this figure show similarity, so the analysis procedure used is adequate.

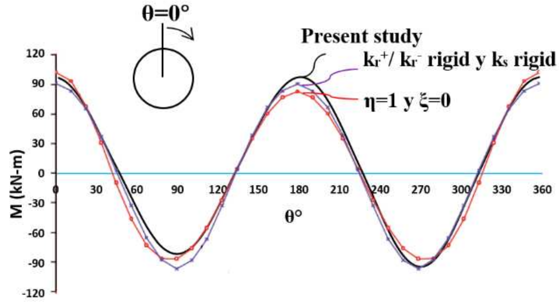

Figure 11. Calibration of the bending moment (Villagrán, 2019).

Figures 12, 13, 14 and 15 show the bending moment along the lining perimeter for all cases analyzed. When comparing the graphs of the mentioned figures, it is observed:

a) In all the graphs a change in trend is observed in the joint position.

b) In each case, the maximum moment corresponds to case I, in $\theta = 90$ degrees or lining top heading, in this case the thickness of soft soil under the tunnel is the smallest, which is congruent with that indicated by Rodríguez (1983), "the most critical condition of analysis is when the tunnel base contacts the hard layer".

c) The maximum- maximum moment corresponds to the case I for 15 year of subsidence, for $\theta = 90$ degrees or lining top heading. In other words, regional consolidation generates increases at the bending moment in the lining and this is more severe for small thicknesses of soft soil under the tunnel.

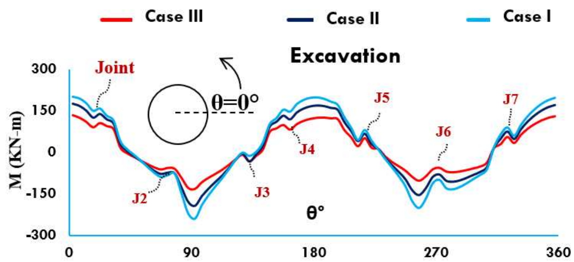

Figure 12. Bending moment along the lining perimeter for all three cases, excavation.

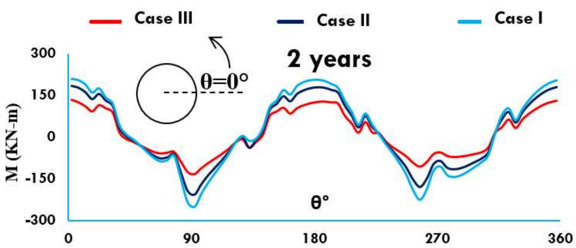

Figure 13. Bending moment along the lining perimeter for all three cases, 2 years.

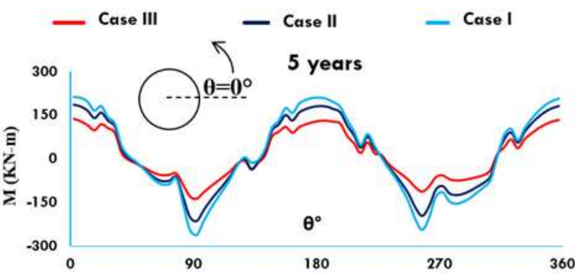

Figure 14. Bending moment along the lining perimeter for all three cases, 5 years.

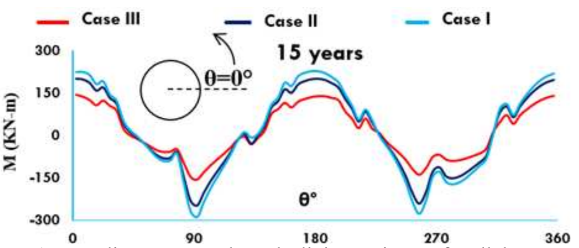

Figure 15. Bending moment along the lining perimeter for all three cases, 15 years.

Figure 16 shows the mean radial stresses (σr) and Figure 17, the tangential stresses (σθ) in the lining. The maximum stresses (σr and σθ) correspond to case I.

Radial stresses: Figure 16 shows that the maximum σr correspond to $\theta = 45$, 135, 225 and 315 degrees, aprox. The minimum σr correspond to $\theta = 90$ degrees and in the lining bottom, the magnitud of σr are little ones.

Tangential stresses: Figure 17 shows that the maximum σθ correspond to $\theta = 0$, 90, 180 and 270 degrees, aprox. The minimum σθ (= 0) correspond to $\theta = 45$, 135, 225 and 315 degrees, approx.

Figures 18 and 19 respectively show the bending moment calculated in the segmented lining along the lining perimeter for the three cases analyzed (excavation stage and for 15 years of subsidence) *versus* the bending moment calculated for uniform ring. The graphs correspond to the odd rings and the even ring. In both Figures 18 and 19, an increase in the bending moment is observed in the area surrounding the joints, mainly when θ = 90 and 270 degrees, approx., that is, at the head and at the bottom of the tunnel lining.

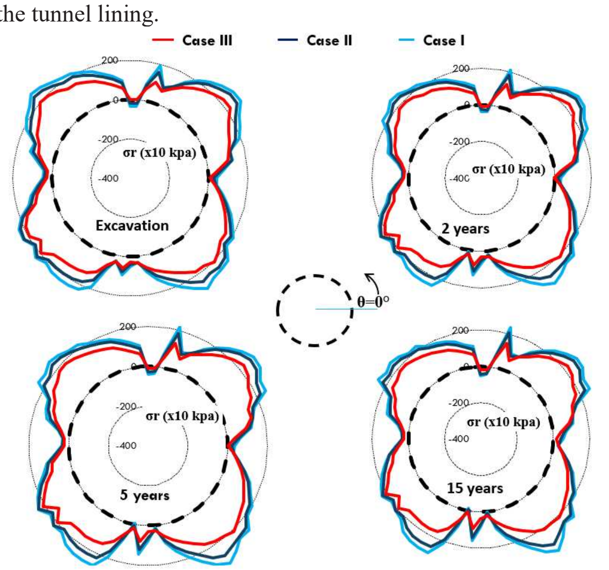

Figure 16. Mean radial stresses (σr) along the lining perimeter for the three cases.

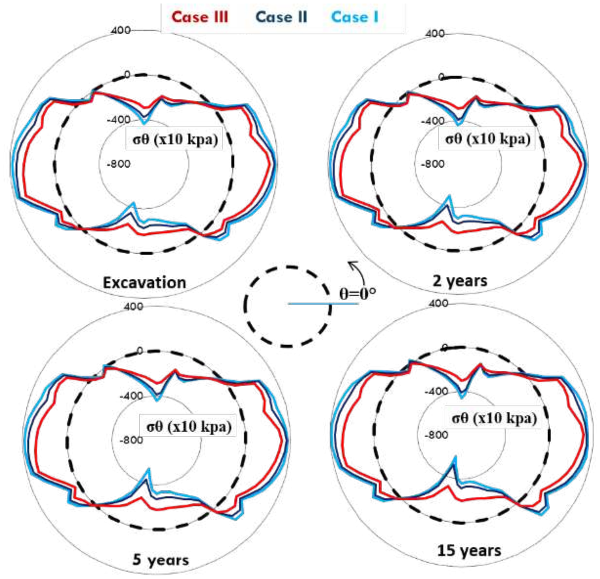

Figure 17. Mean tangential stresses (σθ) along the lining perimeter for the three cases.

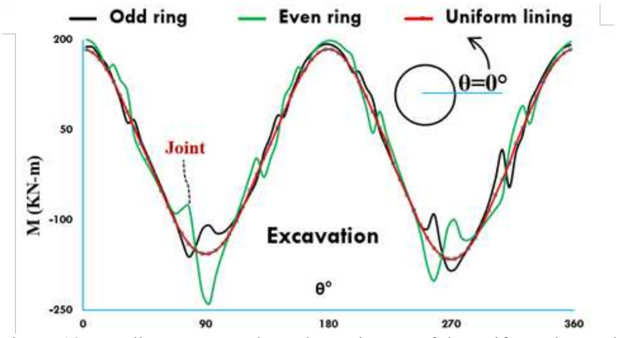

Figure 18. Bending moment along the perimeter of the uniform ring and lining in the presence of joints, excavation.

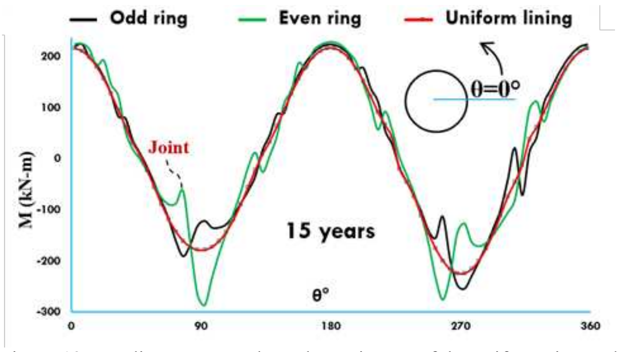

Figure 19. Bending moment along the perimeter of the uniform ring and lining in the presence of joints, 15 years of regional consolidation.

4 CONCLUSIONS

The results of the three-dimensional numerical analysis of finite differences that includes transverse, longitudinal and transition joints (interface elements) of a tunnel with a single segmented lining built in soil in regional consolidation process indicate that:

a) The calculated oval of the lining is congruent with what was observed shortly after (about 2 years) having built the tunnels in soft soil. That is, convergence of the head and bottom of the liner and divergence of the sides of the liner.

b) In addition, the oval of the uniform ring is smaller compared to the oval of the segmented lining, as is logical, due to the reduction in stiffness due to the presence of joints. The results of the present study indicate that, the difference in oval valeu between the segmented lining and the uniform ring, it is a direct function of the opening of the joints present in the segmented lining.

c) There are transfer of mechanical elements (normal and tangential stresses and bending moments) between segments and between rings, with change in the tendency due to the presence of the joints. The distribution and magnitude of the mechanical elements calculated here are comparable with results reported by Zhenchang et al. (2015). In the absence of joints, uniform ring, the bending moment does not present variation in the trend, contrary to the segmental tunnel, because according to Zhenchang, "the bending moment in the longitudinal joint is transferred from one ring to another through the shear mechanism of the transverse joints".

e) For boundary conditions imposed by stiffness changes, zones that do not consolidate, such as the intersection of the tunnel with a station, for example, the translations and rotations between segments and between rings will be important for tunnels with only segmented primary lining.

5 REFERENCES

Auvinet G. and Rodríguez-Rebolledo J.F. 2010. Análisis, diseño, construcción y comportamiento de obras subterráneas en suelos. *XXV Reunión Nacional de Mecánica de Suelos e Ingeniería Geotécnic*a, (págs. 33-42, Volumen I). Acapulco.

Blom C. 2002. Design philosophy of concrete linings for tunnels in soft soils. *Tesis doctoral. Delft University Press*.

Boresi and Schmidt. 2003. Advance mechanics of materials (6a Edición ed.). *John Wiley y Sons*.

Botello J. 2014. Control de asentamientos bajo el túnel inmerso en suelo sometido a subsidencia. *Tesis de maestría. Instituto Politécnico Nacional*, Ciudad de México.

Carrillo *et al*. 2019. Introducción al Método de Diferencias Finitas y su Implememntación Computacional. *Facultad de Ciencias, UNAM*, México.

Comulada-Simpson M. and Maidl. 2010. Diseño y análisis estructural de dovelas en suelos blandos. *Primer simposio Internacional de Túneles y Lumbreras, AMITOS y SMIG*. México.

DAUB. 2013. Recommendations for the design, production, and installation of segmental rings. *Deutscher Ausschuss für unterirdisches Bauen*, 46.

Galván A. 2013. Comportamiento estructural de túneles con dovelas prefabricadas en suelo blando. *Tesis doctoral. Universidad Nacional Autónoma de México*, Ciudad de México.

Hart R. 1993. An introduction to distinct element modeling for rock engineering. *Comprehensive rock engineering: principles, practice and projects*, 17.

Itasca c.g.i. 2011. FLAC3D, Fast Lagrangian Analysis of Continua, User´s Guide. *Itasca Consulting Group Inc.* Minneapolis, Min. USA.

Luttikholt A. 2007. Ultimate Limit State Analysis of a Segmented Tunnel Lining. *Tesis de maestría. Delft University of Technology*. Holanda.

Marti J. and Cundall P. 1982. Mixed Discretization Procedure for Accurate Solution of Plasticity Problems. *Int. J. Num. Methods and Anal. Methods in Geomech*, 12.

Montero E. 2013. Simulación del colapso en túneles dovelados mediante la formación de articulaciones en vigas. *Concreto y Cemento. Investigación y Desarrollo*, 14.

Pacheco J. 2007. Modelo de subsidencia del valle de Querétaro y predicción de agretamientos superficiales. *Tesis doctoral. Universidad Nacional Autónoma de México*. México.

Peña *et al*. 2012. Comportamiento estructural de juntas entre dovelas de concreto. *Redalyc*, 18.

Peña F. and Basurto B. 2013. Factor de reducción de rigidez para túneles dovelados. *3° Simposio Internacional sobre túneles y lumbreras en suelos y roca*. México, D.F., pág. 11.

Pérez M. 2013. Distribución de esfuerzos y desplazamientos alrededor de un túnel circular y en su revestimiento. *Tesis de maestría. Universidad Nacional Autónoma de México*. México.

Rodríguez F. 1983. Esfuerzos internos en túneles circulares. *IDIEM*, 12.

Rodríguez-Rebolledo *et al*. 2012. Análisis y diseño del revestimiento definitivo de túneles en suelos blandos. *2° Simposio Internacional sobre túneles y lumbreras en suelos y roca*, 10.

Salazar J. 2012. Estudios de la interacción entre revestimientos de túneles dovelas. *Tesis de maestría. Universidad Nacional Autónoma de México*. México.

Santoyo E. 2007. Historia y actualidad del hundimiento regional de la Ciudad de México. *TGC*. Recuperado en 2014, p-6.

Sarmiento N. 2011. Análisis tridimensional de la cara de concreto de presas de enrocamiento. *Tesis doctoral. Instituto de Ingeniería, UNAM*. México.

Tunnelling A. I. (2000). Guidelines for the Design of Shield Tunnel Lining. *Tunnelling and underground space technology*, 29.

Villagrán J.M. 2019. Evaluación de la estabilidad de túneles dovelados sometidos a consolidación regional. *Tesis de maestría. Instituto Politecnico Nacional*. México.

Wood D.M. 1990. Soil Behaviour and Critical State Soil Mechanics. *Cambridge: Press Syndicate of the University of Cambridge*.

Wu H.M. Shu Y.M. and Zhu, J.G. 2011. Implementation and verification of interface constitutive model in FLAC3D. *Water Science and Engineering*, 12.

Zhenchang G. 2015. Studies on the key parameters in segmental lining design. *Journal of Rock Mechanics and Geotechnical Engineering*, 10.